International Journal of Astrobiology 2 (3): 155–170 (2003) Printed in the United Kingdom
DOI: 10.1017/S1473550403001629

Precession-driven migration of water in the surficial layers of Mars

Tetsuya Tokano

DLR, Institut für Raumsimulation, 51170 Köln, Germany
e-mail: tetsuya.tokano@dlr.de

Abstract: A linear correlation analysis between the Mars Odyssey neutron fluxes and various surface parameters indicates that the annual maximum surface temperature is the most important factor controlling the soil water content in the surficial (upper few tens of centrimetres) layers of the Martian soil. This is likely to be associated with the higher enthalpy of hydration of minerals in comparison with the enthalpy of sublimation of ice, which is presumably almost absent in the surficial layer. While presently the maximum surface temperature occurs near 30° S because of perihelion in late southern spring, the season of perihelion periodically migrates by virtue of precession. Consequently, the maximum surface temperature as well as the driest place on Mars should move from one hemisphere to the other with a period of about 51 000 yr. A significant amount of surficial (adsorbed) water would then be exchanged between the hemispheres and between the soil and other reservoirs, especially the polar caps and the polar layered deposits, and is probably borne out by the stratigraphic structure of these deposits. It is suggested that the water migration driven by the orbital eccentricity and precession may be as important as the obliquity-driven exchange of water, particularly very close to the surface, where ground ice is unstable.

The zones of liquid water stability oscillate somewhat in a north–south direction in the course of the precession cycle, but are most prevalent in parts of the low and mid northern latitudes as well as in the Hellas Basin. The thermal stability of liquid water tends to be high where the near-surface soil water content is low, indicating that the periodic melting of ground ice by solar heating is not a likely source of liquid water on the surface, but some episodic processes should provide water, if any.

An enhanced soil water content near the surface is always accompanied with a reduced peak ultraviolet flux, both reducing the chemical reactivity of the soil. In the present epoch the northern hemisphere may represent astrobiologically more clement environmental conditions.

Received 1 June 2003, accepted 13 August 2003

Key words: Mars, water.

Introduction

Mars Odyssey Gamma-Ray Spectrometer (GRS) for the first time succeeded in mapping the global distribution of hydrogen (indicative of H_2O) in the shallow subsurface of Mars (Boynton *et al*. 2002; Feldman *et al*. 2002; Mitrofanov *et al*. 2002). One out of many interesting results is that the near-surface soil contains a small, spatially varying amount of H_2O (typically a few wt%) almost everywhere on the planet, in addition to the large ground ice reservoirs in the polar region, which extend up to near the surface. Subsequently, Tokano (2003) suggested that a substantial portion of water in the shallow subsurface at low and mid latitudes may be adsorbed water on mineral grains and that the actual global water distribution near the surface may be a result of the global water cycle in the atmosphere and soil.

There is no reason to believe that the global distribution of subsurface water has been invariant throughout Martian history, even under a present-like cold climate. Previous work has suggested that the global distribution of ground ice may have substantially changed as a result of the obliquity variation of Mars (Fanale *et al*. 1986; Zent *et al*. 1986; Kieffer & Zent 1992; Mellon & Jakosky 1995). At high obliquities ground ice extends to lower latitudes than today because the annual-mean subsurface temperature decreases. The astronomically forced climate change on Mars in analogy with the terrestrial Milankovitch cycle has recently been demonstrated by the observation of the stratigraphic structure of the northern polar layered terrains (Laskar *et al*. 2002). However, it was shown that not only the obliquity, but also another astronomical parameter manifests itself in the stratigraphic structure, i.e. the climatic precession cycle which has a shorter period (approximately 51 000 yr). This effect is caused by a combination of the precession of the spin axis of Mars (with a period of 1.7×10^5 yr) and the precession of the axis to the orbital plane (with a period of 7×10^4 yr), which causes the migration of the season at which perihelion occurs. The season of perihelion dictates whether and how strong the north–south asymmetry of the global insolation pattern becomes.

As already mentioned, the impact of the precession cycle on the Martian climate is best demonstrated in the stratigraphic structure of the north polar layered deposits (Laskar *et al.* 2002), but have also been investigated theoretically in some other studies. Mellon & Jakosky (1992) predicted that the precession cycle is able to change the annual mean surface temperature by a few kelvin, with a larger variation at higher latitudes. The mean surface temperature in the northern hemisphere generally becomes higher when the perihelion passage occurs near $L_S = 90°$. In the ground ice evolution model of Mellon & Jakosky (1995) the precession cycle was one forcing mechanism for the advance and recession of the ground ice, together with the obliquity oscillation. The orbital eccentricity was shown to cause a slight north–south asymmetry in the global subsurface temperature distribution and ground ice distribution, but was not considered as significant as the variation caused by the obliquity cycle. By means of a general circulation model (GCM) Fenton & Richardson (2001) investigated whether the season of perihelion would alter the surface wind directions, but they found that this is not the case. The reason for this result was assumed to be the global elevation difference, which is sufficient to keep the global circulation pattern invariant with respect to the precession cycle. Similarly, Haberle *et al.* (2003) found in their GCM study that the season of perihelion can cause significant differences in the magnitude of various wind systems, but the basic global pattern of surface stress and lifting of dust for a given obliquity seems to be relatively insensitive to the longitude of perihelion.

Previous work came to the conclusion that there is a relationship between the orbital parameters and the global ice distribution on the surface and in the subsurface. The present study will show that a similar relationship may also apply to low latitudes, where ground ice is presumably unstable and absent.

Correlation between the soil water content and surface parameters

The presence or absence of ground ice is primarily controlled by the mean soil temperature and the atmospheric vapour content (Paige 1992; Mellon & Jakosky 1993, 1995). In contrast to this, the soil humidity in ice-free soil can depend on various factors such as temperature, vapour pressure, the adsorptive capacity of the soil or the efficiency of water transport/exchange between the soil and the atmosphere (Tokano 2003). Prior to an assessment of the global water distribution in the past, a more systematic analysis of the relationship between the soil water content and various surface parameters is presented here. For this purpose the correlation coefficient between the soil water content and various surface parameters that may or may not be relevant for the soil humidity is calculated based on global maps acquired by remote sensing or predicted by recent models.

Table 1. *Correlation coefficient between the surface parameters and the neutron fluxes measured by Mars Odyssey GRS*

Parameter	Fast[1]	Epithermal[1]	Fast[2]	Epithermal[2]
Topography	0.443	−0.081	0.206	−0.081
Albedo	−0.374	−0.290	−0.304	−0.241
Thermal inertia	−0.116	0.118	0.022	0.143
Mean surface temperature	0.780	0.700	0.739	0.619
Maximum surface temperature	0.824	0.448	0.596	0.360
Minimum surface temperature	0.372	0.434	0.398	0.387
Mean meridional wind speed	−0.028	−0.016	−0.020	−0.011

[1] HEND (Mitrofanov *et al.* 2002).
[2] Neutron spectrometer (Feldman *et al.* 2002).

The leakage flux of neutrons produced in the soil by galactic cosmic rays and slowed down by collision with hydrogen may be regarded as a measure for the soil water content in the upper few metres of the soil (Boynton *et al.* 2002; Feldman *et al.* 2002; Mitrofanov *et al.* 2002). The larger the depression of epithermal and fast neutrons, the larger the water content is in the soil. However, the relationship between the soil water content and neutron fluxes is not linear, particularly if the vertical profile of the water content is not uniform. Since fast neutrons originate from shallower depth than epithermal neutrons, the fast neutron data are more indicative of the water content very close to the surface as compared with epithermal neutron data. For the data analysis the leakage neutron flux data acquired by the Mars Odyssey High Energy Neutron Detector (HEND) and Neutron Spectrometer in late northern winter on Mars published in Mitrofanov *et al.* (2002) and Feldman *et al.* (2002), respectively, are used. The data files are available as part of the Special Products in the 2001 Mars Odyssey Data Archives at NASA Planetary Data System (PDS).

The correlation coefficient between each of these neutron fluxes and the surface parameter under consideration (topography, albedo, thermal inertia, annual mean, maximum and minimum surface temperature, near-surface meridional wind speed) is calculated and shown in Table 1. The topography data are those acquired by the Mars Orbiter Laser Altimeter (MOLA) of Mars Global Surveyor (MGS) (Smith *et al.* 2001), the albedo and thermal inertia data from the Thermal Emission Spectrometer (TES) of MGS (Mellon *et al.* 2000). The data sets themselves have been extracted for this study from the European Mars Climate Database (Lewis *et al.* 1999). Also the mean, maximum and minimum surface temperatures and the mean meridional wind speed are calculated with the data from the same database.

Topography

The fast neutrons indicative of the hydrogen abundance in the surficial layer of Mars show a moderate correlation with the topography, while the epithermal neutrons representative

https://doi.org/10.1017/S1473550403001629 Published online by Cambridge University Press

of a thicker layer show almost no correlation with the topography. This means that the near-surface water content tends to be higher at deeper places on Mars. A possible explanation for this behaviour may be the fact that lower places generally exhibit a higher water vapour pressure because of the thicker atmospheric column (Tokano 2003). On the other hand, the negligible correlation between the topography and epithermal neutron fluxes indicates that the variable vapour pressure has little effect on the water content in deeper layers.

Albedo

The surface albedo shows a moderate anti-correlation with both fast and epithermal neutron fluxes. The water content is thus higher in high-albedo regions. Obviously, high-albedo regions absorb less solar flux than low-albedo regions, so at a given latitude the surface temperature remains lower than in low-albedo regions, allowing a larger amount of adsorbed water in the surficial soil.

At the same time, the albedo differences themselves are likely to be related to differences in surface mineralogy and dust coverage. Spectral mapping indicates that in the low-albedo regions pyroxenes, plagioclase feldspars are prevalent, while the high-albedo regions generally do not display significant mineral concentrations but are extensively covered by dust (Bandfield 2002). However, it is important to note that the global albedo pattern can change within only a few decades. For instance, the formerly dark Cerberus region has brightened significantly since Viking observations (James *et al*. 1996).

Thermal inertia

The thermal inertia exhibits a rather low correlation with the neutron fluxes, although some correlation is apparent at low latitudes if one analyses the longitudinal distribution. For instance, there is a clear correlation in Arabia Terra between the depressed neutron fluxes (high water content) and the low thermal inertia (Tokano 2003). The overall poor correlation between the thermal inertia and soil humidity may reflect the complexity the thermal inertia is representing. The thermal inertia is known to vary with the soil particle size (Presley & Christensen 1997), but also with the degree of cementation, for example, by salts (Jakosky & Christensen 1986). As the particle size is correlated with the specific surface area of minerals and hence the adsorbed water holding capacity, some correlation between the particle size and adsorbed water content is possible. The thermal inertia in turn affects the surface temperature and its diurnal amplitude. As a whole, the thermal inertia does not seem to be a primary factor controlling the soil water content on Mars.

Surface temperature

More promising is the correlation between the surface temperature and neutron fluxes. The annual mean surface temperature exhibits a relatively high correlation (>0.6) with all of the neutron fluxes, particularly with the fast neutron fluxes. The soil water content clearly decreases with increasing mean surface temperature. This is straightforward because the ground ice thermal stability decreases with temperature as shown in previous work (e.g. Paige 1992; Mellon & Jakosky 1993). However, this correlation also applies to low latitudes where no ground ice is expected to exist near the surface. This suggests that the surface temperature is controlling the adsorbed water content as well.

The highest correlation (0.824) among all parameters is that between the annual maximum surface temperature (Fig. 1) and fast neutron fluxes acquired by HEND (Fig. 2 of Mitrofanov *et al*. 2002). The maximum surface temperature shown here is quite similar to that predicted by another GCM (Fig. 4 of Haberle *et al*. 2001). The highest maximum surface temperature is found in the latitudinal belt between the equator and 30° S because the perihelion occurs in late southern spring when the Sun at local noon is ahead in this region. Within this belt the absolute maximum occurs south of Tharsis Montes near Solis Planum (30° S, 120° W).

Since the HEND fast neutrons are most indicative of the uppermost soil layer, this correlation indicates that there is a strong link between the maximum surface temperature and the water content in the soil very close to the surface. Such a behaviour was observed in the global water cycle model of Tokano (2003) in which a higher summer peak temperature in the south gave rise to a stronger desiccation than elsewhere. This strongly indicates that the input of high energies is controlling the water content very close to the surface. The most likely explanation for this behaviour is the high hydration (adsorption) enthalpy of many hydrous minerals in comparison with the enthalpy of condensation or sublimation of water. In the ice-free near-surface regolith the hydration/dehydration of minerals rather than sublimation/condensation of ice changes the soil water content.

Another implication is that hydration and dehydration is occurring in the temperature range within which the annual maximum temperature varies on Mars (220–310 K, see Fig. 3 later). The dehydration curve is characteristic of the hydrous mineral under consideration, but one of the minerals that substantially hydrate and dehydrate in this temperature range is Na-clinoptilolite, which belongs to the zeolites (Bish *et al*. 2003). At a typical vapour pressure on the Martian surface (1.5×10^{-6} bar) the fractional water content in Na-clinoptilolite is ~0.8 at 230 K and ~0.4 at 300 K, for instance. Thus a variation by a factor of 2 or more would be possible on the Martian surface.

The correlation between the mean surface temperature and neutron fluxes is also relatively high (a correlation coefficient of at least 0.6), but not as high as between the maximum temperature and the HEND fast neutron fluxes. However, concerning the epithermal neutron fluxes the correlation is better than with the maximum surface temperature. This difference means that in the deeper layer the mean (rather than the maximum) surface temperature is a more important factor for the soil water content. The global map of the mean surface temperature is more symmetric about the equator, with a maximum at the equator and a steady decrease with latitude. Finally, the annual minimum surface temperature

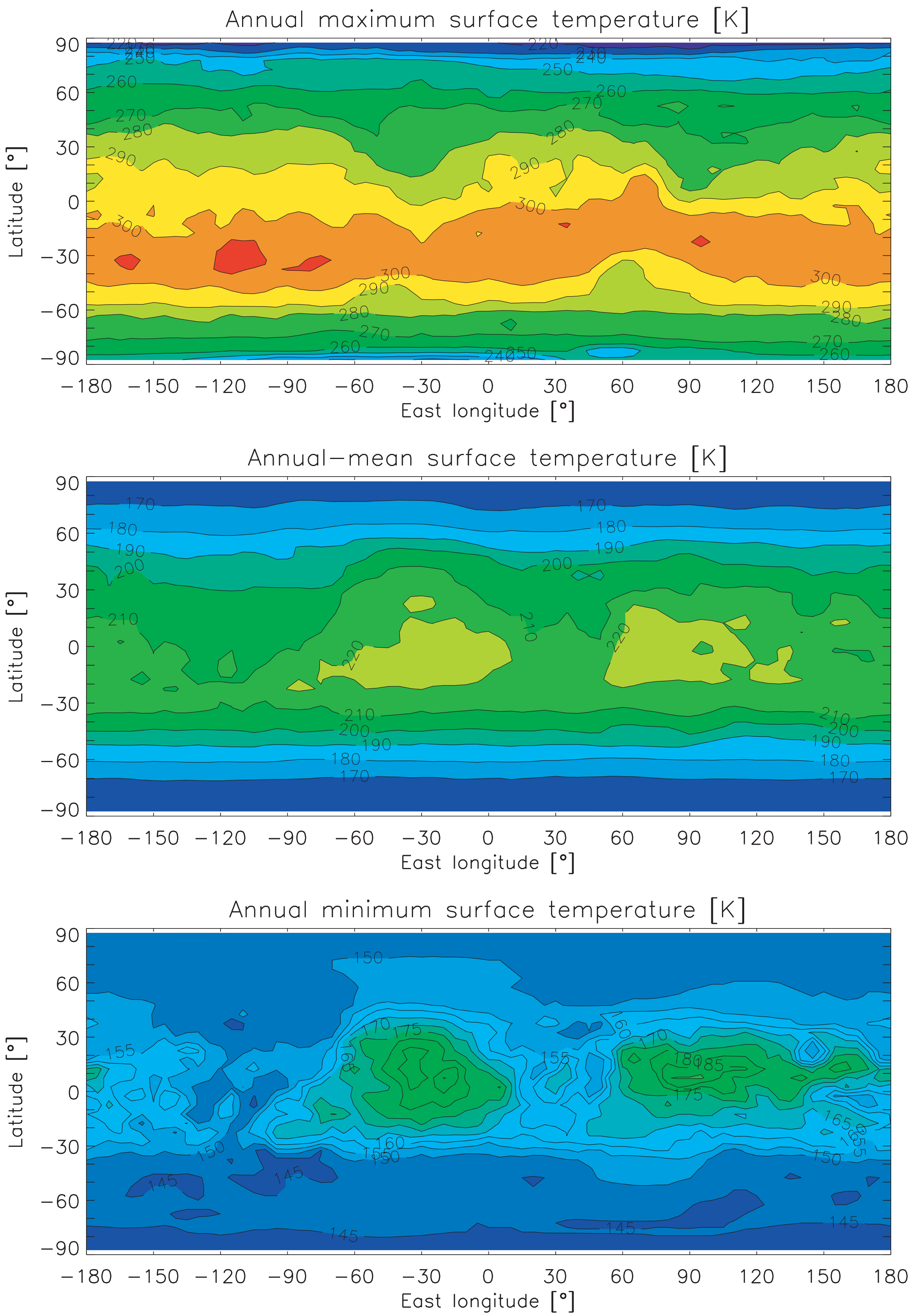

Fig. 1. Global map of the annual maximum, mean and minimum surface temperature under the present climate extracted from the European Mars Climate Database (Lewis *et al.* 1999) for the standard dust scenario (Mars Global Surveyor Dust Scenario, January 2001). The maximum surface temperature best correlates with the HEND fast neutron fluxes data (Table 1).

https://doi.org/10.1017/S1473550403001629 Published online by Cambridge University Press

has a lower correlation with both fast and epithermal neutron fluxes. This low correlation indicates that the condensation of volatiles in winter is virtually irrelevant to the soil water content, in contrast to the surface frost deposition.

Mean meridional wind speed

Water vapour near the surface is subject not only to possible exchange with the subsurface, but also to advective transport by the prevailing wind. Moreover, the surface exchange or sublimation of surface frost depends on the wind speed near the surface. Meridional wind is essential for the global, interhemispheric transport of water vapour. Therefore, the correlation between the near-surface (5 m above the surface) meridional wind speed averaged over one Martian year extracted from the European Mars Climate Database (Lewis *et al.* 1999) and the neutron fluxes has also been calculated.

It turns out that the overall correlation between the neutron fluxes and the wind speed is very poor, so we may conclude that the wind is not an important factor for the near-surface soil water content. Particularly windy regions ($|v| > 10$ m s^{-1}) year-around include Isidis Planitia (10° N, 90° E), parts of Arabia Terra (20° N, 50° E), Solis Planum (20° S, 100° W) and Tyrrhena Terra (20° S, 90° E), but they comprise both wet and dry areas.

Soil water content variation in the past

Model description

The most important message of the previous section and Table 1 is the likelihood of a more or less linear relationship between the leakage fast neutron flux and the annual maximum surface temperature. If so, the annual maximum temperature could be used as a measure for the surface water content to be expected for each epoch. As the insolation pattern changes secularly, the surface temperatures and the near-surface soil water content ought to change as well.

The temporal variation of the soil moisture is maintained by the global water cycle, i.e. desiccation of the soil at places becoming hotter, global vapour transport in the atmosphere and moistening of the soil at places becoming colder (Tokano 2003). This study tacitly assumes that such a global water cycle has always existed. The variation of the orbital parameters is slow enough that there should be abundant time for adsorbed water near the surface to be exchanged with the atmosphere. The basic assumption of this model study is thus that the global distribution of the near-surface soil water content can be approximately predicted by calculating the surface temperature. The adsorptive capacity of the soil not only depends on the soil temperature, but also on the mineral morphology, but on the timescales of 10^4–10^5 yr we are considering, that are short in geological terms, the surface mineralogy is unlikely to have greatly changed in the absence of abundant liquid water on the surface.

The model to be described here predicts the temporal evolution of the annual maximum surface temperature at all grid points through one recent precession cycle. The global distribution of the near-surface water content to be expected under these maximum surface temperatures is estimated subsequently.

Surface temperature

The surface temperature T_S is predicted by the combined force–restore method after Dickinson (1988),

$$\frac{\partial T_S}{\partial t} = \frac{1}{C_g}\left[\frac{S_0(1-A)}{r^2}\cos\zeta - f\varepsilon\sigma T_S^4\right] + \frac{2\pi}{P_d}(T_a - T_S) \qquad (1)$$

and

$$\frac{\partial T_a}{\partial t} = -\frac{2\pi}{\sqrt{P_a P_d}}(T_a - T_S) + \frac{2\pi}{P_a}(T_c - T_a). \qquad (2)$$

In Eq. (1) the first term on the right-hand side is the solar flux absorbed by the surface, the second term is the net thermal flux emitted by the surface and the third term is the heat conduction to the subsurface. Equation (2) predicts the seasonally varying diurnal-mean subsurface temperature T_a at the diurnal skin depth (intermediate layer). Here, the terms on the right-hand side are the heat conduction between the surface and intermediate layer as well as between the intermediate and deep layer (annual skin depth, with constant temperature T_c), respectively. C_g is the specific heat capacity per unit area, $S_0 = 1370$ W m^{-2} is the solar constant, A is the surface albedo, r is the instantaneous (true) Sun–Mars distance, ζ is the solar zenith angle, $f = 0.93$ is the thermal flux reduction associated with the CO_2 greenhouse effect at 6 hPa (François *et al.* 1990), ε is the surface emissivity and $\sigma = 5.67 \times 10^{-8}$ W m^{-2} K^{-4} is the Stefan–Boltzmann constant. $P_d = 88\,643$ s is the diurnal period and $P_a = 5.927 \times 10^7$ s is the annual period. The specific heat capacity per unit area is $C_g = 0.5I(P_d/\pi)^{1/2}$, where I is the thermal inertia. The astronomical calculation of r and ζ are given in the Appendix. The equations are solved with a constant timestep interval of 30 min.

The albedo A and thermal inertia I data are those derived from TES (Mellon *et al.* 2000), and are extracted for this study from the European Mars Climate Database (Lewis *et al.* 1999). The emissivity ε is set to unity (Mellon *et al.* 2000).

In the model it is assumed that the mean atmospheric pressure and composition remain constant and no substantial exchange of atmospheric CO_2 with other possible reservoirs took place during the period under consideration (51 000 yr). The main reason for this assumption is that the north polar stratigraphic structure is consistent with the prevalence of a present-like thin atmosphere (Laskar *et al.* 2002) as well as the suggestion that the southern polar cap could not provide a much thicker CO_2 atmosphere in other epochs because it is mainly composed of H_2O ice rather than CO_2 ice (Byrne & Ingersoll 2003). Therefore, an extreme periodic change of the Martian climate by an inherent variability as considered by Yokohata *et al.* (2002) is not taken into account in this study. Consequently, the surface albedo is kept constant at the present value at each place since no perennial surface frost exists in this assumption outside the polar region. The albedo change of the polar cap is ignored given the small areal extension compared with the rest of the planet.

Strong planet-encircling dust storms lowers the daytime surface temperature in summer by about 5 K compared with a dust-poor year (Smith *et al.* 2002). This may also affect the annual maximum temperature since dust storms develop in the hottest season. However, this effect is neglected in this model because the dust storm strength undergoes significant interannual variability and hence is almost unpredictable. As we are searching for the maximum temperature within a timescale of decades and centuries, it is sufficient to simulate a dust-free, hot year, which should occur sometimes within this timescale.

Soil water content

In the fast neutron map of HEND (Mitrofanov *et al.* 2002) the moist polar region was inferred to have a soil water content of 5 wt% in the upper layer at a normalized neutron flux of 0.54 and the driest place (Solis Planum) a presumable water of 0.25 wt% with a normalized neutron flux of 1 (0.15 count s^{-1}). Viking 1 site (22° N, 48° W) was assumed to have a water content of 1 wt%, based on an *in situ* measurement by the Gas Chromatograph-Mass Spectrometer (GCMS) (Biemann *et al.* 1977). In the southern hemisphere typical water contents in the upper dry layer were 1 wt% at 42° S and 2 wt% at 62° S (Boynton *et al.* 2002). The assumption in this study is that the annual maximum surface temperature scales linearly with the fast neutron flux and inversely with the soil water content in the uppermost layer (a few tens of centimetres) of the subsurface, given the high linear correlation between these parameters as shown in Table 1. Any expression can only be a rough estimate. The reference value of 1 wt% at the Viking 1 landing site itself is a rough estimate because the water content measurement by the GCMS suffered from several deficiencies, and a water content of 2 wt% cannot be ruled out for this site (Biemann *et al.* 1977).

The water content in the shallow subsurface is expressed as a function of the annual maximum surface temperature. The function is meant to approximately reconcile with the observational constraints,

$$w(T_{max}) = -15\frac{T_{max}}{T_{max,\mathbf{0}}} + 15.25 \qquad (3)$$

where $w(T_{max})$ is the soil water content (in wt%), T_{max} is the annual maximum surface temperature at a given place and $T_{max,\mathbf{0}} = 311$ K is the same at Solis Planum (30° S, 270° E) under the present climate.

Results

Annual maximum surface temperature

Fig. 2 shows for five different longitudes of perihelion in the past the seasonal and latitudinal variation of the solar flux absorbed by the surface at local noon. The figure shows the zonal-mean distribution, so the albedo and thermal inertia have been zonally averaged in the calculation. Presently the perihelion is at $L_S = 251°$ in late southern spring, so the annual maximum insolation is found in this season at low southern latitudes. The season of perihelion passage always shifts to later seasons. Some 11 000 years ago the perihelion was at the northern autumnal equinox ($L_S = 180°$), so on an annual average the insolation pattern was symmetric about the equator and the maximum insolation occurred at the equator. During this and the present epoch the location of maximum insolation has shifted southward and will continue to do so for a further 2950 years from now.

The secular variation of the annual maximum surface temperature for each latitude is shown in Fig. 3. The hottest place on Mars is currently found near 30° S. During the last 25 000 years the hottest place on Mars slowly migrated from the low northern latitudes to the present place, but will shift further southward in the future. 25 000 years ago the low southern latitudes had a summer peak temperature about 20 K colder than now. The secular variation of the maximum temperature is observed not only at low latitudes, but extends up to the polar region. In the near past the northern polar region/southern polar region has been warmer/colder than at present, respectively. This is consistent with the evolution of the summer peak insolation in the northern polar region predicted by Laskar *et al.* (2002) and Edvardsson *et al.* (2002). An approximate symmetry above the equator was found when the perihelion was near $L_S = 0°$ or 180°, i.e. some 11 000 or 39 000 yr before present. The slightly lower peak temperature in the northern hemisphere is ascribed to the generally higher albedo, which gives rise to a smaller amount of absorbed solar energy for a given insolation pattern. During this period the obliquity also changed to some extent. For instance, the obliquity 52 900 yr before present was 22.7° in comparison with the present 25.18°, so the maximum surface temperature at that time occurred at a slightly equatorward latitude compared with today, but the difference is not significant.

Soil water content

As a result of significant spatial and temporal variation of the maximum surface temperature the soil water content near the surface undergoes a substantial change. In this study the soil water content refers to all types of water, but dominantly to adsorbed water because ground ice is unstable near the surface. The soil water content depends primarily on latitude. It is generally low in warm regions and continuously decreases towards cold regions (Fig. 4). However, since the maximum temperature is found presently at low southern latitudes rather than at the equator the minimum soil water content occurs between 20° S and 30° S, in agreement with the Mars Odyssey data. The model predicts the soil water content in this area to be less than 0.5 wt%. Outside this area the water content gradually increases towards both poles. Some hemispheric asymmetry remains: while the latitudinal gradient is larger in the southern hemisphere, the total increase in the soil water content is larger in the northern hemisphere (up to 4.5 wt% at the north pole). The layer under consideration here is the dry upper layer above the presumable ground ice deposits.

https://doi.org/10.1017/S1473550403001629 Published online by Cambridge University Press

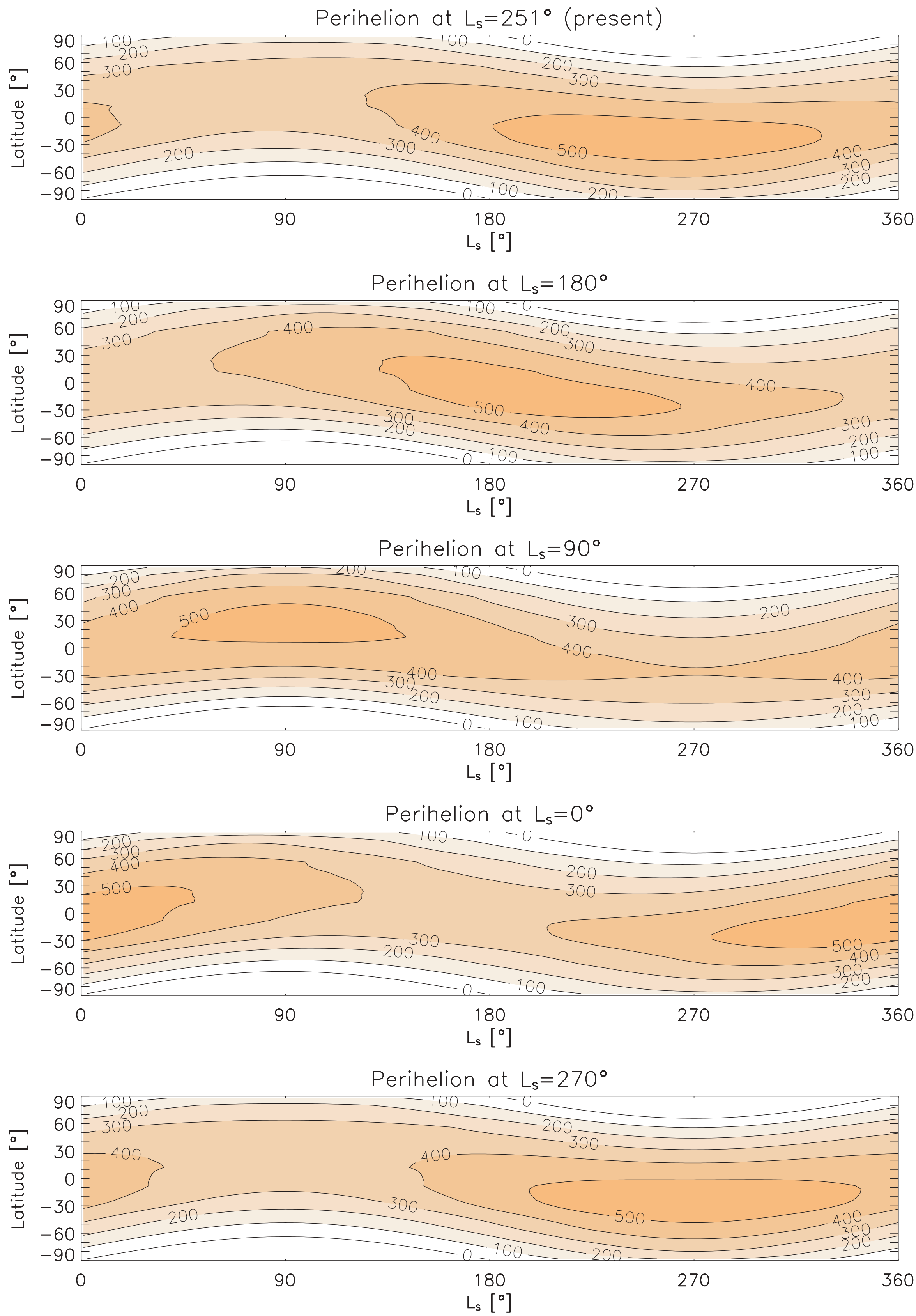

Fig. 2. Latitudinal and seasonal variation of the zonal-mean solar flux absorbed by the Martian surface (in W m^{-2}) at local noon at five different seasons of perihelion during the last precession cycle.

https://doi.org/10.1017/S1473550403001629 Published online by Cambridge University Press

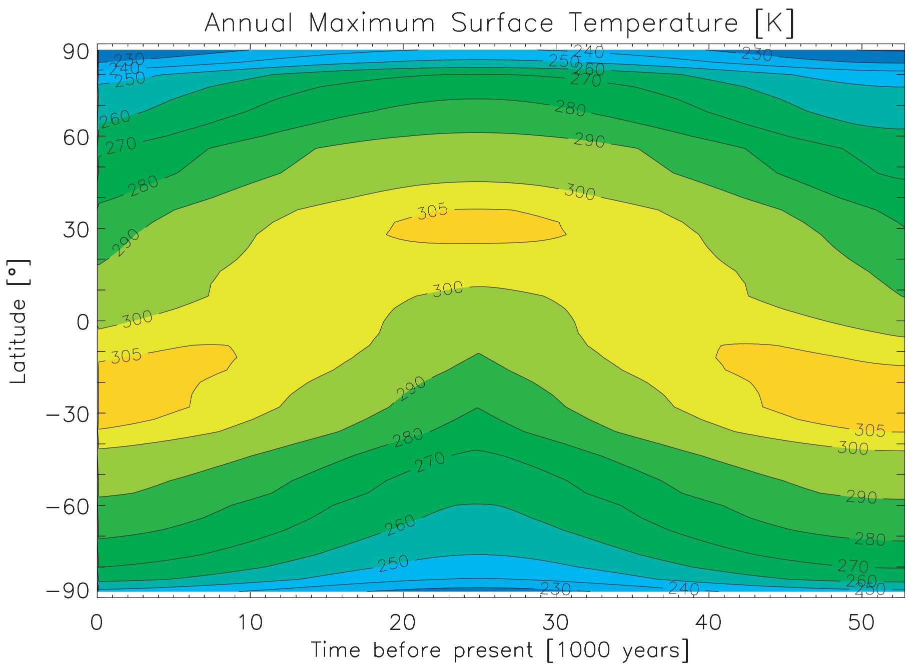

Fig. 3. Latitudinal and temporal variation of the zonal-mean annual maximum surface temperature through the last climatic precession cycle predicted by the model. The variable longitude of perihelion is $L_S = 250.99°$ at present, but was $L_S = 180°$ at 11.0 kyr, $L_S = 90°$ at 25.0 kyr, $L_S = 0°$ at 38.9 kyr and $L_S = 270°$ at 52.9 kyr before the present.

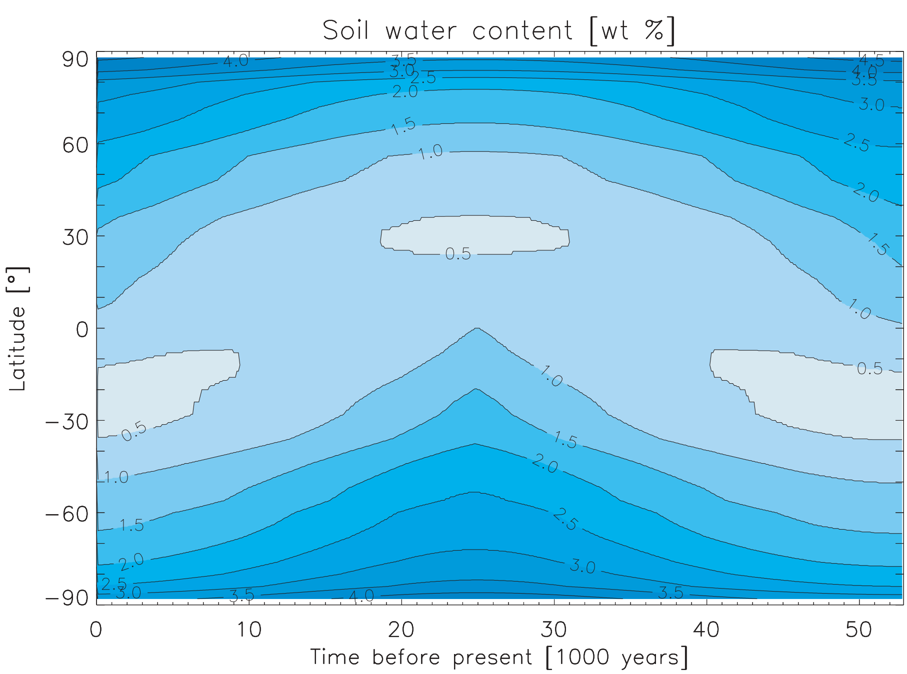

Fig. 4. Same as Fig. 3 for the near-surface soil water content.

During the last 25 000 years the region of minimum water content slowly migrated from 30° N to the present position in the south, and this migration would continue in the next 2950 years until the perihelion passage arrives at $L_S = 270°$. The north–south migration of the water near the surface is likely to take place via the atmosphere rather than by horizontal motion within the soil. The soil becomes slowly desiccated in regions where the soil is becoming warmer in high summer, released water molecules migrate to the atmosphere, are transported by the global circulation and enter the subsurface in the opposite hemisphere, where the soil is becoming cooler in summer. In this way the water content at 30° S decreased from 1.5 wt% to less than 0.5 wt%, while at 30° N the situation was reversed. This model thus illustrates that the soil over the entire planet should undergo a repeated cycle of desiccation and

https://doi.org/10.1017/S1473550403001629 Published online by Cambridge University Press

moistening over timescales of 50 000 yr, irrespective of the thermal stability of ground ice.

The global map of the soil water content at different epochs (Fig. 5) shows further variability in the longitudinal direction, especially at low latitudes, where the albedo and thermal inertia variations are large. In comparison with deeper layers, where the soil water content varies between 1 wt% and >35 wt% (Boynton *et al.* 2002; Feldman *et al.* 2002; Mitrofanov *et al.* 2002), the spatial variability near the surface is generally small, indicating the absence of ice-cemented regolith in this depth range. However, considering the large area occupied by the low latitudes, the small water content (without ice) may still represent a significant exchangeable water reservoir.

At low and mid latitudes the upper panel of Fig. 5 does not coincide well with the contour of global maps of the ground ice distribution of Mellon & Jakosky (1993, 1995). The most obvious discrepancy is found near the equator: in the region between 0° and 50° W the ground ice stability is lowest planetwide (Mellon & Jakosky 1995), while according to Fig. 5 the near-surface soil water content here is higher than in the surroundings. This difference can be explained by the fact that for the ground ice stability the *mean* surface temperature is crucial, while for the adsorbed water content near the surface the *maximum* surface temperature is of foremost importance. In the above-mentioned area the mean surface temperature is relatively high but the maximum surface temperature is low because of the high thermal inertia.

When the perihelion was at $L_S = 90°$ (northern summer solstice), the global map displays a reversed hemispheric asymmetry with a generally drier northern hemisphere. Longitudinal variation is also discernible in this epoch. Within the latitude belt around 30° N the driest places are found near 60–90° W (northeast of Tharsis), 150–180° W (Amazonis Planitia) and 0–60° E (Arabia Terra). These regions are characterized by a high albedo and low thermal inertia, and fall to Unit A according to Mellon *et al.* (2000). Both Viking 1, Viking 2, Pathfinder and Beagle 2 (Isidis Planitia) landing sites are inferred to have been drier at that time compared with the present. The longitudinal variation in the southern hemisphere is generally smaller than in the north, probably reflecting the fact that the old southern highlands are more homogeneous with respect to albedo and thermal inertia. During a perihelion passage at $L_S = 0°$ (northern vernal equinox), the global map becomes, not surprisingly, more symmetric about the equator.

An intercomparison of the three maps indicates that presently the soil water content in the north/south is higher/lower than the average, respectively. Nevertheless, some regions on Mars remain wetter than elsewhere on average. This is best recognized at low latitudes where there is a marked longitudinal variation. The region covering the debouchment of the outflow channels and Chryse Planitia (0–30° N, 0–60° W), Isidis Planitia to Elysium (90–150° E) is relatively wet. On the other hand, relatively dry regions include Syrtis Major Planum (10° N, 60° E), Kasei Valles (30° N, 60° W) and a part of Amazonis Planitia (30° N, 180° W).

A visual comparison of Fig. 5 with the global map representing different thermal inertia-albedo modes (Fig. 7 of Mellon *et al.* 2000) yields that Unit B generally contains more water than elsewhere at low latitudes. Unit B is characterized by a high thermal inertia and low albedo. In general, the correlation of these units with geological or geomorphic units was found to be sporadic (Mellon *et al.* 2000). This is no discrepancy since the thermal properties (albedo and thermal inertia) are sensitive to the uppermost few centimetres, which are not necessarily correlated with the bedrock geology.

Fig. 6 shows the temporal variation of the hemispherically and globally integrated mass of soil water in the uppermost 1 m of the soil. It is readily seen that currently the northern hemisphere contains twice as much water as the southern hemisphere. During the last 20 000 years the northern hemisphere has become wetter because the southern hemisphere continued to desiccate at the expense of the northern hemisphere, in agreement with the global water cycle model of Tokano (2003). This trend may continue for the next 2950 years until the perihelion passage arrives at $L_S = 270°$. When the perihelion passage takes place in northern summer, the maximum temperature is lower in the southern hemisphere, so the soil humidity is higher in the south.

The exchange of water is not restricted to between the hemispheres. The variation of the global sum of water in the shallow subsurface by $\sim 10^{16}$ kg (corresponding to an equivalent water depth of 10 cm) over timescales of about 20 000 years indicates that an exchange with other water reservoirs must take place. Presently the subsurface is gaining water at the expense of other reservoirs with a rate of 7×10^{10} kg yr^{-1} globally. The immediate source of water should be the atmospheric water vapour. As the total atmospheric water abundance is of the order of 10^{12} kg (Smith 2002), the atmosphere could indeed account for such a source. However, since the atmospheric water is fed by the polar caps, the exchange ultimately should be between the polar caps and the soil, with the atmosphere being only a medium.

This implication may indeed be borne out by the stratigraphic structure of the northern polar layered deposits analysed by Laskar *et al.* (2002). In this analysis a high correlation between the summer peak insolation at the north pole and a high brightness of the northern polar layered deposits was recognized at the period of the climatic precession cycle (25.4 arcsec yr^{-1}). Under the assumption that the high brightness is caused by an enhanced deposition of H_2O ice, this could mean that water dehydrated from the soil of the northern hemisphere is deposited at the north pole during an epoch in which the summer peak insolation increases in the northern hemisphere. With an approximate area of the northern polar layered deposits of $\sim 10^{12}$ m^2 and the total amount dehydrated from the soil of $\sim 1.5 \times 10^{16}$ kg (Fig. 6), the exchange of water between the northern soil and the northern cap would result in an ice deposit thickness of about 16 m during a climatic precession cycle or a deposition

https://doi.org/10.1017/S1473550403001629 Published online by Cambridge University Press

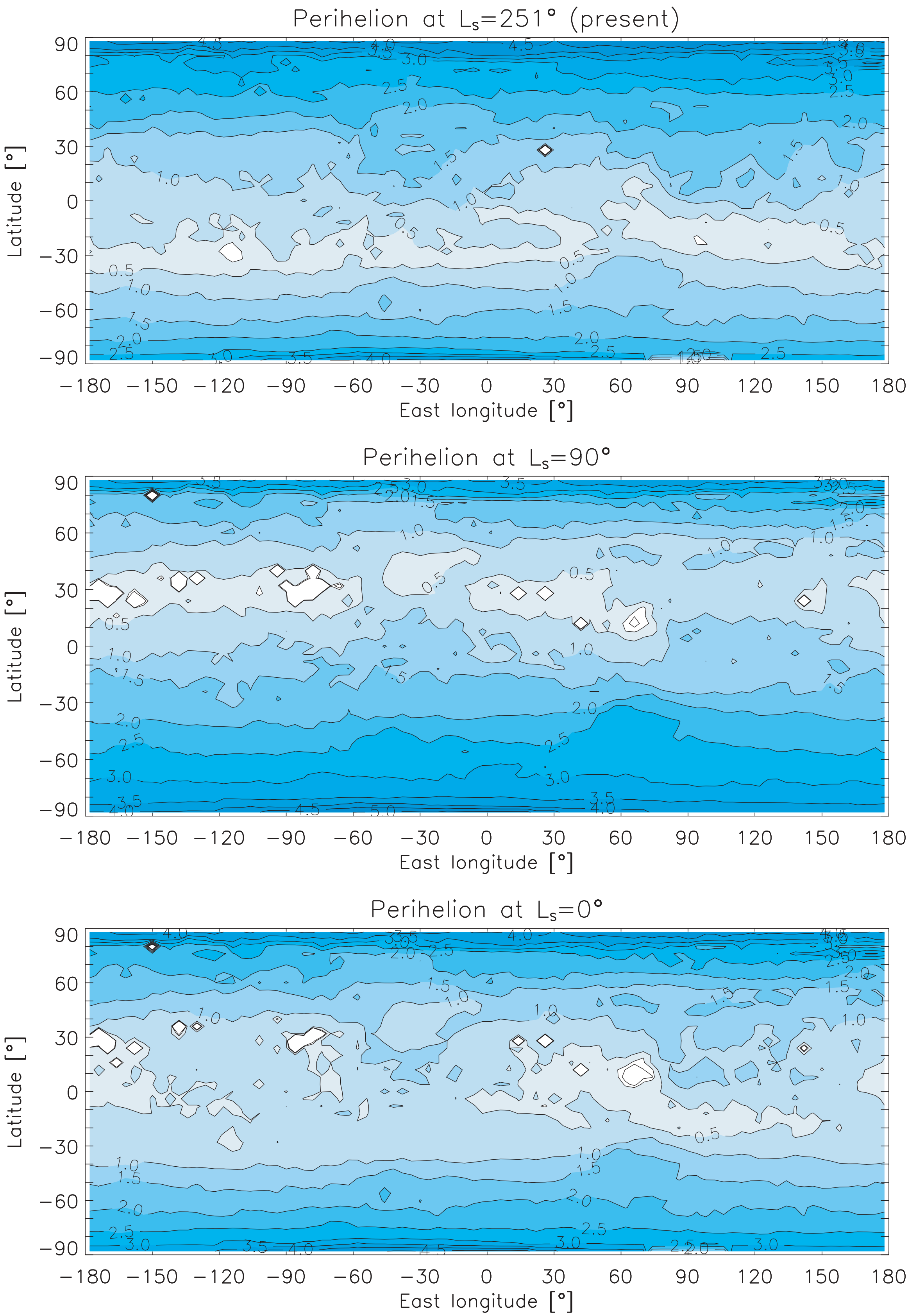

Fig. 5. Global map of the near-surface soil water content in wt% for the present season of perihelion, perihelion at the northern summer solstice ($L_S = 90°$) and perihelion at the northern vernal equinox ($L_S = 0°$). Contour lines are plotted at 0.2, 0.5, 1, 1.5, 2, 2.5, 3, 3.5, 4, 4.5 and 5 and brighter shading corresponds to lower water contents.

https://doi.org/10.1017/S1473550403001629 Published online by Cambridge University Press

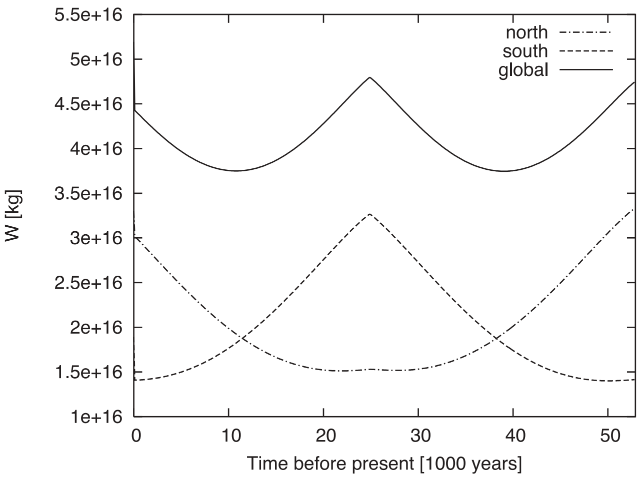

Fig. 6. Temporal evolution of the total soil water content in the uppermost 1 m through the last climatic precession cycle. The sums are calculated for the northern hemisphere, southern hemisphere and the entire planet (global).

rate of 0.07 cm yr^{-1}. This agrees well with the average deposition rate of 0.05 cm yr^{-1} estimated by Laskar *et al.* (2002). Also the orbiter observations indicating a net annual loss of water from the northern polar cap in the present epoch (Haberle & Jakosky 1990) is consistent with the result of this model, suggesting a net gain of water in the soil of the northern hemisphere at the expense of other reservoirs (north pole).

At this place it is meaningful to discuss the obvious hemispheric asymmetry concerning the atmospheric water abundance (Smith 2002) and polar caps (Clifford *et al.* 2000). Observations discern that both water vapour and polar cap H_2O ice are more abundant in the northern hemisphere than in the southern hemisphere. It now turns out that this hemispheric asymmetry also applies to the surficial soil humidity. Houben *et al.* (1997) suggested that the orbital eccentricity may be ultimately responsible for the asymmetric distribution of water on Mars. On the other hand, Richardson & Wilson (2002) proposed that the Hadley circulation, which is responsible for the global transport of water vapour in the atmosphere, may always be stronger in southern summer because of the general elevation difference between the north and south, causing a wetter northern hemisphere throughout history. However, as shown earlier the linear correlation between the near-surface wind speed and the near-surface soil water content is tiny in comparison with other surface parameters, particularly the annual maximum surface temperature, so the meridional wind (Hadley circulation) is unlikely to be a primary factor controlling the near-surface soil moisture. Also the correlation of the soil water content with the topography is smaller than with the maximum or mean surface temperature. As the surface temperature variation is to a first approximation astronomically forced, the general behaviour displayed in Fig. 6 can hardly be discarded, and it is suggested that the periodic variation of the north–south asymmetry of the soil water content at low and mid latitudes is likely to occur on timescales of 50 000 years.

The continuous presence of adsorbed water near the surface, with some periodic variation, may contribute to hydrolytic surface weathering of the soil at an extremely slow rate by virtue of the surface potential exerted by the solid as suggested by Banin (1996). Moreover, the repeated cycle of hydration/dehydration in combination with chemical reactions of sulphates and oxides may cause a crust formation of the soil over long timescales (Jakosky & Christensen 1986; Bishop *et al.* 2002). For the duricrust formation no liquid water or ice would be required. A monolayer of adsorbed water would be sufficient to move the salt ions (Jakosky & Christensen 1986). By this mechanism sulphate components may be transported to the surface (Bishop *et al.* 2002). The hydration and dehydration was suggested primarily in the context of the Martian obliquity cycle, but basically the water migration associated with the precession cycle should cause a similar effect.

Liquid water stability on the surface

The secular variation of the surface temperature would have an important consequence for the stability of liquid water on the surface as well. Haberle *et al.* (2001) and Lobitz *et al.* (2001) searched by a GCM and spacecraft data, respectively, for places on Mars where the surface temperature and pressure meet the minimum requirements for liquid water according to the phase diagram (temperature and pressure above the triple point but below the boiling point). They came to the conclusion that the most favourable places for liquid water are located in the Hellas and Argyre Basin at southern mid latitudes and a large portion between the equator and 40° N. Much of the applicable places are found to coincide with the locales of Amazonian paleolakes identified by Cabrol & Grin (2001). The absolute age of most Amazonian paleolakes has been constrained to 400–600 Myr. Although this age for the paleolakes is geologically recent, several thousand obliquity cycles and 10^4 climatic precession cycles have passed since then. The simulation of Haberle *et al.* (2001) was carried out for the present climate and it is worth considering how the situation may have changed throughout the precession cycle.

In order to investigate this question, a simulation analogous to Haberle *et al.* (2001) is carried out. The model calculates for every latitudinal grid point the length of time during a Mars year where the instantaneous surface temperature and surface pressure are above the triple point (273.15 K, 6.11 hPa) but below the boiling point, which is pressure-dependent and is determined by the saturation vapour pressure. The effect of freezing point depression by salts has been ignored for simplicity because we are only interested in the general trend. Since the obliquity is virtually unchanged and hence the seasonal amplitude of the surface pressure is unlikely to increase, the surface pressure at a given place is kept at the present mean value, regardless of the season of perihelion.

Fig. 7 shows the model results for three representative epochs within a precession cycle. The result for the present epoch is similar to that obtained by a GCM by Haberle *et al.* (2001). The maximum length of liquid water stability is found

https://doi.org/10.1017/S1473550403001629 Published online by Cambridge University Press

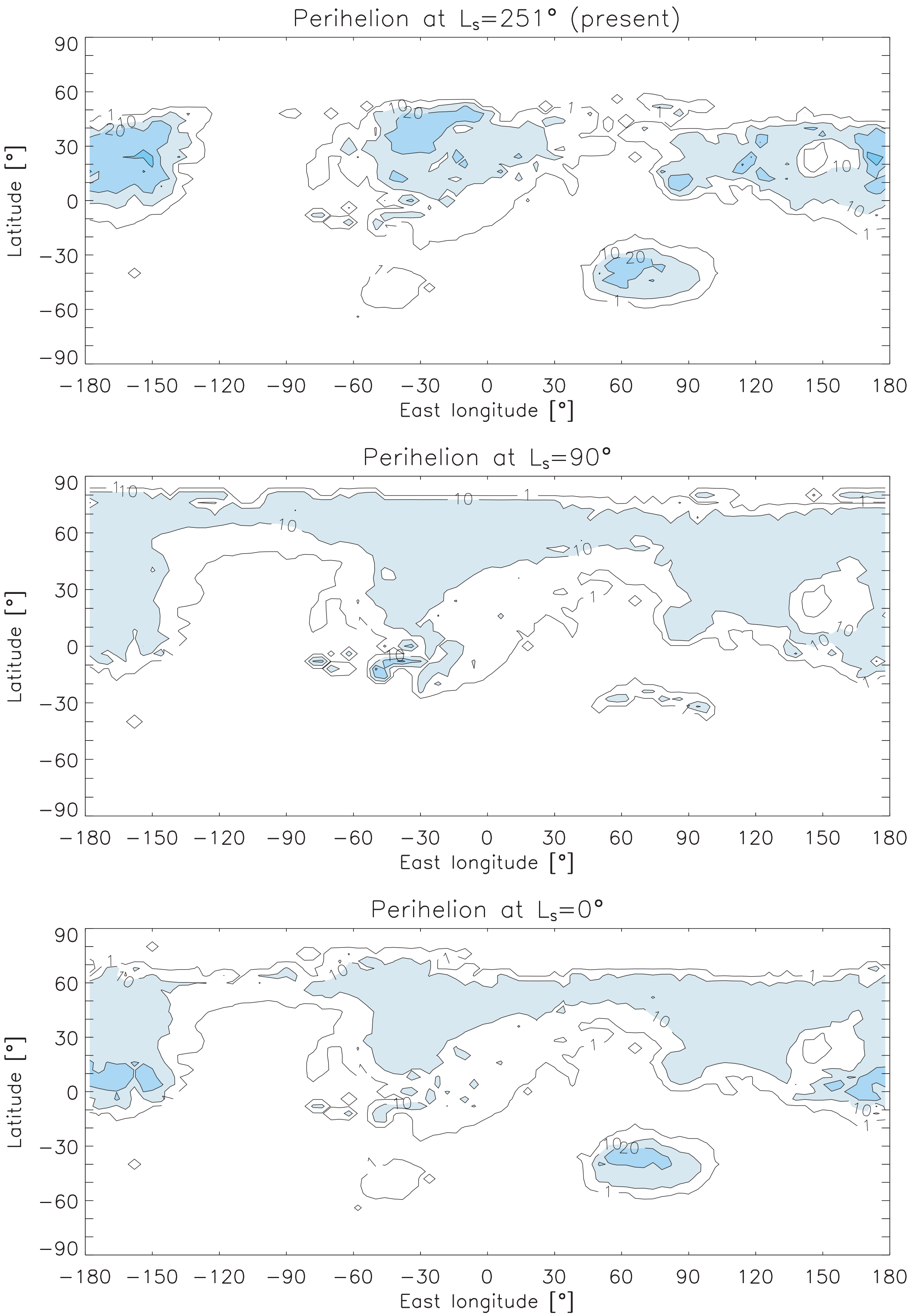

Fig. 7. Global map showing the length of time during a Mars year (sols) where the surface temperature and surface pressure are above the triple point of water but below the boiling point. Results are shown for the present season of perihelion ($L_S=251°$), perihelion at the northern summer solstice ($L_S=90°$) and perihelion at the northern vernal equinox ($L_S=0°$).

https://doi.org/10.1017/S1473550403001629 Published online by Cambridge University Press

at 20–30° N, 160° W west of Olympos Mons in the southeastern part of Amazonis Planitia with more than 40 sols per Mars year. Other maxima are found in the Hellas Basin, Chryse Planitia near 30° N, 30° W, sporadically in Utopia Planitia and between Isidis Planitia and Elysium. With the exception of the Hellas Basin all of these regions are located at low northern latitudes.

When the perihelion occurs at $L_S = 90°$, the pattern changes qualitatively. Since the maximum temperature in the southern hemisphere drops and barely exceeds the triple point, liquid water stability in the Hellas Basin drastically decreases. The equatorial canyon systems are the only regions in the southern hemisphere where the stability increases. In general the northern hemisphere becomes more conducive to liquid water, at least for 10 sols per Mars year. Remarkably, the regions with an enhanced liquid water stability nicely correlate with the northern lowlands where an ocean is suspected to have existed in the Hesperian (e.g. Carr & Head 2003). On the other hand, the correlation with the Amazonian paleolakes identified by Cabrol & Grin (2001) is poor. This is in stark contrast to the present epoch in which the correlation with these paleolakes is found to be good (Haberle *et al.* 2001). When the perihelion passage occurs at $L_S = 0°$ the liquid water stability is highest in the Hellas Basin and in the southern rim of Amazonis Planitia (0–10° N, 180° W), but not in Chryse Planitia or Utopia Planitia.

This result illustrates that the thermal condition favouring the existence of liquid water on the surface of Mars may substantially change over timescales of 50 000 years, even in the recent past. There are also regions where liquid water is never stable because of the low surface pressure such as a large portion of the southern hemisphere or the mountainous regions in the northern hemisphere.

The highest liquid water stability throughout the precession cycle is achieved in the Hellas Basin, southern rim of Amazonis Planitia, Chryse Planitia and southeast of Elysium. With the exception of the Hellas Basin, liquid water stability is always higher in the northern hemisphere. Amazonian paleolakes of the Hellas Group and Oxia Palus Group coincide with the zones of most favourable liquid water sites, while some other lake groups such as the Mangala Group or the Maja Group are outside these zones.

The presence of liquid water not only requires the right temperature and pressure range at the surface, but also the availability of abundant H_2O at these places at the right time. It turns out that the condition favourable for liquid water is not accompanied with a high soil water content near the surface as is evident from an intercomparison of Figs 5 and 7. The soil water content near the surface decreases with increasing summer temperature, while the stability of liquid water generally increases. This may indicate that the periodic melting of near-surface ground ice in summer does not appear to be a viable mechanism for the formation of liquids on the surface, in agreement with the suggestion that the likely origin of water in Amazonian paleolakes is either hydrothermal, aquifer discharge, sapping or precipitation (Cabrol & Grin 2001). The occasional existence of liquid water on the surface may be rather independent of the soil water content in the topmost few tens of centimetres, but more susceptible to atmospheric or geological processes.

As a whole the presence of liquid water on the surface is more favourable in the northern hemisphere throughout the precession cycle and particularly when the perihelion passage occurs in northern summer. The basic reason for this hemispheric bias is the higher surface pressure in the north.

Astrobiological implication

The uppermost 1 m of the Martian soil analysed in this study is generally not considered a favourite niche for hypothetical microbial life because of the extreme ultraviolet (UV) irradiation, highly oxidizing compounds (e.g. superoxides) in the soil and lack of liquid water, so extant or extinct microbial life, if any, is expected in deep subsurface sediments (Ellery *et al.* 2003). In particular, the lack of liquid water in these layers, with possible rare local and temporal exceptions, may provide the most problematic factor. Nevertheless, it is meaningful to consider the possible astrobiological consequence of the periodic hydration and dehydration of the near-surface soil discussed in this study.

The distribution of organics in the soil is intimately related to the chemical reactivity, the possible mechanisms of which are summarized in Zent *et al.* (2003). Some of the proposed mechanisms are influenced by the water abundance in the soil. If the release of O_2 in the Viking Gas Exchange Experiment was caused by catalytic decomposition of an unstable oxidizing material by H_2O, the concentration of the oxidants may correlate negatively with the H_2O abundance (Zent & McKay 1994). At the same time the present model study indicates that the peak insolation and hence also the peak UV flux at the surface generally is anti-correlated with the soil water content near the surface. This means that presently the concentration of oxidants should be lower in the northern hemisphere for two reasons (low peak UV flux and high water content). Alternatively, the high soil reactivity may be due to superoxides (O_2^-) that would readily form under Martian conditions, particularly under extremely low water vapour concentration (Yen *et al.* 2000). In the presence of water, superoxide ions decompose. Hence, the superoxide concentration and the water content may be anti-correlated.

Regardless of the exact nature of the chemical reactivity, the reactivity at depth is thought to decline exponentially with depth. In regions with an enhanced adsorbed water content the degree of oxidation may decline more rapidly with depth than other regions because of the less effective oxidant diffusion into the soil (Ellery *et al.* 2003). In the present epoch the northern hemisphere receives less peak insolation (and also UV flux) and contains more water in the soil, particularly at high latitudes, providing a more favourable environmental condition. In other words, one might encounter in the northern hemisphere organic material at shallower depth in comparison with the south. The same can be stated for high latitudes in comparison with equatorial latitudes. This situation obviously changes during the course of a climatic precession cycle and there are repeatedly epochs during which the southern hemisphere becomes more clement.

The duricrust formation as a result of repeated cycles of hydration and dehydration of the near-surface soil in combination with chemical reactions (Bishop *et al.* 2002) itself may be of astrobiological relevance. Clark (1998) suggested that the duricrust on Mars may be a preferred habitat for near-surface, soil-dwelling biota because it is indicative of vertical material transport.

Conclusions

The global water cycle modelling by Tokano (2003) in concert with the presumable subsurface water distribution inferred by Mars Odyssey give rise to considering the factors responsible for the spatial and possibly temporal variability of the subsurface water distribution. The linear correlation between the fast and epithermal neutron flux measured by Mars Odyssey GRS (Feldman *et al.* 2002; Mitrofanov *et al.* 2002) and various surface parameters have been analysed. These parameters comprise the topography (and hence surface pressure), surface albedo, thermal inertia, annual maximum, mean and minimum surface temperature and the meridional wind speed near the surface. Modest correlation with the neutron fluxes does exist for topography and albedo, but the best correlation (>0.8) is found between the HEND fast neutron fluxes and the annual maximum surface temperature. This result indicates that the soil water content near the surface (the uppermost few tens of centimetres) is primarily controlled by the maximum surface temperature in summer. The main reason for this behaviour is probably the high enthalpy of hydration of minerals in comparison with the enthalpy of sublimation of ice, indicating the presence of adsorbed water rather than ice in the near-surface soil of Mars.

Previous work has focused on the secular migration of ground ice by obliquity change because the thermal stability of ground ice depends on the mean soil temperature. However, the above correlation analysis points out the importance of the summer peak temperature for the water content in the ice-free shallow subsurface. The maximum surface temperature is presently found near 30° S because perihelion occurs near the southern summer solstice, but the warmest places are likely to oscillate between the northern and southern hemisphere on geologically short timescales. The basis for this assumption is the astronomical theory, which predicts secular variation of the insolation pattern with variable orbital parameters of Mars (obliquity, eccentricity and season of perihelion). Among these parameters the climatic precession cycle is the shortest one (51 000 yr), and is evidenced in the stratigraphical structure of the northern polar layer deposits (Laskar *et al.* 2002).

A numerical simulation of the variation of the annual maximum surface temperature and soil water content near the surface has been carried out for the last climatic precession cycle. Over the entire globe the maximum surface temperature varies by up to 30 K over roughly 50 000 years with a periodic reversal of the hemispheric asymmetry. The soil becomes desiccated in areas with increasing summer peak temperature and becomes moister where the situation is reversed. The migration of water between the hemisphere is likely to take place via the atmosphere. The total amount of water stored in the shallow subsurface also varies with time. Currently, slow desiccation is taking place at low and mid southern latitudes, while the northern hemisphere is becoming wetter, and in total the soil is gaining water at the expense of other water reservoirs, particularly the polar caps and the polar layered deposits. The observed stratigraphic structure of these deposits seem to confirm such an exchange.

Some regions of the planet sustain relatively more surficial water than other regions throughout the precession cycle. It turns out that water-richer areas are preferentially found in areas denoted as Unit B according to the global map of Mellon *et al.* (2000) representing the different modes of thermal inertia and albedo. Unit B is characterized by a high thermal inertia and low albedo. The global distribution of water near the surface may differ significantly from that in somewhat deeper soil, where the mean soil temperature is more important for the water abundance.

The stability of liquid water on the surface of Mars also changes with the season of perihelion. When the perihelion passage occurs in northern summer, most parts of the northern lowlands are conducive to liquid water for a dozen of sols per Mars year, while in the southern hemisphere liquid water is almost everywhere unstable. Perihelion in southern summer causes the liquid water stability regions to shift southward. Some distinct places within the northern and southern low and mid latitudes then exhibit an enhanced stability. On the average deep basins and plains at low latitudes are the most favourable places for the occasional presence of liquid water because of the simultaneous high surface pressure and high temperature.

However, regions with an enhanced liquid water stability are more desiccated than other regions. Therefore, water stored near the surface and hence the periodic melting of ground ice is generally not a likely source of liquid water on the surface. This suggestion does not preclude the presence of other water sources considered by, for example, Cabrol & Grin (2001).

The repeated cycle of hydration and dehydration may contribute to the long-term formation of duricrust by allowing salt ions to migrate toward the surface. It may be of astrobiological importance that an enhanced soil water content near the surface is always accompanied with a reduced peak UV flux. In the present epoch the northern hemisphere may be providing more clement environmental conditions, at least with respect to water availability and radiation.

Appendix. Astronomical parameters

The true Sun–Mars distance r is primarily a function of season, but varies secularly

$$r = \frac{a(1 - e^2)}{(1 + e \cos\theta)} \tag{A1}$$

where $a = 1.523\,68$ AU, e is the orbital eccentricity and θ is the longitude of perihelion. e (presently 0.0934) is variable, and is adopted from Laskar *et al.* (2002).

θ, the key parameter in this study, is given by

$$\theta = 360^\circ - \lambda_p - L_S \tag{A2}$$

where λ_p is the argument of perihelion and L_S is the areocentric longitude of the Sun (season on Mars).

The argument of perihelion λ_p is presently 250.99° in late southern spring, but varies (Allison & McEwen 2000) as

$$\lambda_p = 250.99^\circ + 0.6447^\circ \text{ century}^{-1}. \tag{A3}$$

The cosine of the solar zenith angle is

$$\cos\zeta = \sin\varphi \sin\delta + \cos\varphi \cos\delta \cos h, \tag{A4}$$

where φ is the latitude on Mars, δ is the solar declination calculated as $\delta = \sin^{-1}(\sin\Theta \sin L_S)$ and h is the hour angle. Here, Θ is the obliquity of Mars, which is 25.189° at present. The exact value of Θ for each epoch is adopted from Laskar *et al.* (2002).

Acknowledgements

The author was supported by the DLR Project Life in Permafrost. He thanks Jacques Laskar for providing the data file on the orbital parameters of Mars. Computational resources were provided by the SSC Karlsruhe.

References

Allison, M. & McEwen, M. (2000). A post-Pathfinder evaluation of areocentric solar coordinates with improved timing recipes for Mars seasonal/diurnal climate studies. *Planet. Space Sci.* **48**, 215–235.

Bandfield, J.L. (2002). Global mineral distributions on Mars. *J. Geophys. Res.* **107** (E6), doi:10.1029/2001JE001510.

Banin, A. (1996). The missing crystalline minerals in Mars soil. *Adv. Space Res.* **18**, 233–240.

Biemann, K. *et al.* (1977). The search for organic substances and inorganic volatile compounds in the surface of Mars. *J. Geophys. Res.* **82**, 4641–4658.

Bish, D.L., Carey, J.W., Vaniman, D.T. & Chipera, S.J. (2003). Stability of hydrous minerals on the Martian surface. *Icarus* **164**, 96–103.

Bishop, J.L., Murchie, S.L., Pieters, C.M. & Zent, A.P. (2002). A model for formation of dust, soil, and rock coatings on Mars: physical and chemical processes on the Martian surface. *J. Geophys. Res.* **107**, 5097, doi:10.1029/2001JE001581.

Boynton, W.V. *et al.* (2002). Distribution of hydrogen in the near-surface of Mars: evidence for subsurface ice deposits. *Science* **297**, 81–85.

Byrne, S. & Ingersoll, A.P. (2003). A sublimation model for Martian south polar ice features. *Science* **299**, 1051–1053.

Cabrol, N.A. & Grin, E.A. (2001). The evolution of lacustrine environments on Mars: is Mars only hydrologically dormant? *Icarus* **149**, 291–328.

Carr, M.H. & Head, J.W. III (2003). Oceans on Mars: an assessment of the observational evidence and possible fate. *J. Geophys. Res.* **108**, 5042, doi:10.1029/2002JE001963.

Clark, B.C. (1998). Surviving the limits to life at the surface of Mars. *J. Geophys. Res.* **103**, 28 545–28 555.

Clifford, S.M. *et al.* (2000). The state and future of Mars polar science and exploration. *Icarus* **144**, 210–242.

Dickinson, R.E. (1988). The force–restore method for surface temperature and its generalizations. *J. Climate* **1**, 1086–1097.

Edvardsson, S., Karlsson, K.G. & Engholm, M. (2002). Accurate spin axes and solar system dynamics: climatic variations for the Earth and Mars. *Astron. Astrophys.* **384**, 698–701.

Ellery, A., Kolb, C., Lammer, H., Parnell, J., Edwards, H., Richter, L., Patel, M., Romstedt, J., Dickensheets, D., Steele, A. & Cockell, C. (2003). Astrobiological instrumentation for Mars – the only way is down. *Int. J. Astrobiol.* **1**, 365–380.

Fanale, F.P., Salvail, J.R., Zent, A.P. & Postawko, S.E. (1986). Global distribution and migration of subsurface ice on Mars. *J. Geophys. Res.* **67**, 1–18.

Feldman, W.C. *et al.* (2002). Global distribution of neutrons from Mars: results from Mars Odyssey. *Science* **297**, 75–78.

Fenton, L.K. & Richardson, M.I. (2001). Martian surface winds: intensity to orbital changes and implications for aeolian processes. *J. Geophys. Res.* **106**, 32 885–32 902.

François, L.M., Walker, J.C.G. & Kuhn, W.R. (1990). A numerical simulation of climate changes during the obliquity cycle on Mars. *J. Geophys. Res.* **95**, 14 761–14 778.

Haberle, R.M. & Jakosky, B.M. (1990). Sublimation and transport of water from the north residual polar cap of Mars. *J. Geophys. Res.* **95**, 1423–1437.

Haberle, R.M., McKay, C.P., Schaeffer, J., Cabrol, N.A., Grin, E.A., Zent, A.P. & Quinn, R. (2001). On the possibility of liquid water on present-day Mars. *J. Geophys. Res.* **106**, 23 317–23 326.

Haberle, R.M., Murphy, J.R. & Schaeffer, J. (2003). Orbital change experiments with a Mars general circulation model. *Icarus* **161**, 66–89.

Houben, H., Haberle, R.M., Young, R.E. & Zent, A.P. (1997). Modeling the Martian sasonal water cycle. *J. Geophys. Res.* **102**, 9069–9083.

Jakosky, B.M. & Christensen, P.R. (1986). Global duricrust on Mars – analysis of remote-sensing data. *J. Geophys. Res.* **91**, 3547–3559.

James, P.B., Bell, J.F. III, Clancy, R.T., Lee, S.W., Martin, L.J. & Wolff, M.J. (1996). Global imaging of Mars by Hubble Space Telescope during the 1995 opposition. *J. Geophys. Res.* **101**, 18 883–18 890.

Kieffer, H.H. & Zent, A.P. (1992). Quasi-periodic climate change on Mars. In *Mars*, eds Kieffer, H.H., Jakosky, B.M., Snyder, C.W. & Matthews, M.S., pp. 1180–1218. University of Arizona Press, Tuscon, AZ.

Laskar, J., Levrard, B. & Mustard, J.F. (2002). Orbital forcing of the Martian polar layered deposits. *Nature* **419**, 375–377.

Lewis, S.R., Collins, M., Read, P.L., Forget, F., Hourdin, F., Fournier, R., Hourdin, C., Talagrand, O. & Huot, J.-P. (1999). A climate database for Mars. *J. Geophys. Res.* **104**, 24 177–24 194.

Lobitz, B., Wood, B.J., Averner, M.A. & McKay, C.P. (2001). Use of spacecraft data to derive regions on Mars where liquid water would be stable. *Proc. Natl Acad. Sci., USA* **98**, 2132–2137.

Mellon, M.T. & Jakosky, B.M. (1992). The effects of orbital and climatic variations on Martian surface heat flow. *Geophys. Res. Lett.* **19**, 2393–2396.

Mellon, M.T. & Jakosky, B.M. (1993). Geographic variations in the thermal and diffusive stability of ground ice on Mars. *J. Geophys. Res.* **98**, 3345–3364.

Mellon, M.T. & Jakosky, B.M. (1995). The distribution and behavior of Martian ground ice during past and present epochs. *J. Geophys. Res.* **100**, 11 781–11 799.

Mellon, M.T., Jakosky, B.M., Kieffer, H.H. & Christensen, P.R. (2000). High-resolution thermal inertia mapping from the Mars Global Surveyor Thermal Emission Spectrometer. *Icarus* **148**, 437–455.

Mitrofanov, I., Anfimov, D., Kozyrev, A., Litvak, M., Sanin, A., Tret'yakov, V., Krylov, A., Shvetsov, V., Boynton, W., Shinohara, C., Hamara, D. & Saunders, R.S. (2002). Maps of subsurface hydrogen from the High-Energy Neutron Detector. *Science* **297**, 78–81.

Paige, D.A. (1992). The thermal stability of near-surface ground ice on Mars. *Nature* **356**, 43–45.

Presley, M.A. & Christensen, P.R. (1997). The effect of bulk density and particle size sorting on the thermal conductivity of particulate materials under Martian atmospheric pressures. *J. Geophys. Res.* **102**, 9221–9229.

Richardson, M.I. & Wilson, R.J. (2002). A topographically forced asymmetry in the Martian circulation and climate. *Nature* **416**, 298–301.

Smith, M.D. (2002). The annual cycle of water vapor on Mars as observed by the Thermal Emission Spectrometer. *J. Geophys. Res.* **107**, 5115, doi:10.1029/2001JE001522.

Smith, M.D. *et al.* (2001). Mars Orbiter Laser Altimeter (MOLA): experiment summary after the first year of global mapping of Mars. *J. Geophys. Res.* **106**, 23 689–23 722.

Smith, M.D., Conrath, B.J., Pearl, J.C. & Christensen, P.R. (2002). Thermal Emission Spectrometer observations of Martian planet-encircling dust storm 2001A. *Icarus* **157**, 259–263.

Tokano, T. (2003). Spatial inhomogeneity of the Martian subsurface water distribution: implication from a global water cycle model. *Icarus* **164**, 50–78.

Yen, A.S., Kim, S.S., Hecht, M.H., Frant, M.S. & Murray, B. (2000). Evidence that the reactivity of the Martian soil is due to superoxide ions. *Science* **289**, 1909–1912.

Yokohata, T., Odaka, M. & Kuramoto, K. (2002). Role of H_2O and CO_2 ices in Martian climate changes. *Icarus* **159**, 439–448.

Zent, A.P. & McKay, C.P. (1994). The chemical reactivity of the Martian soil and implications for future missions. *Icarus* **108**, 146–157.

Zent, A.P., Fanale, F.P., Salvail, J.R. & Postawko, S.E. (1986). Distribution and state of H_2O in the high-latitude shallow subsurface of Mars. *Icarus* **67**, 19–36.

Zent, A.P., Quinn, R.C., Grunthaner, F.J., Hecht, M.H., Buehler, M.G., McKay, C.P. & Ricco, A.J. (2003). Mars atmospheric oxidant sensor (MAOS): an in-situ heterogeneous chemistry analysis. *Planet. Space Sci.* **51**, 167–175.